Title: Pharmacokinetics, Brain Distribution and Plasma Protein Binding of Carbamazepine and Nine Derivatives: New Set of Data for Predictive in Silico ADME Models

Author: Ana Fortuna Gilberto Alves Patrício Soares-da-Silva Amílcar Falcão

PII: S0920-1211(13)00218-0
DOI: http://dx.doi.org/doi:10.1016/j.eplepsyres.2013.08.013
Reference: EPIRES 4989

To appear in: *Epilepsy Research*

Received date: 5-4-2013
Revised date: 29-6-2013
Accepted date: 8-8-2013

Please cite this article as: Fortuna, A., Alves, G., Soares-da-Silva, P., Falcão, A., Pharmacokinetics, brain distribution and plasma protein binding of carbamazepine and nine derivatives: new set of data for predictive in silico ADME models, *Epilepsy Research* (2013), http://dx.doi.org/10.1016/j.eplepsyres.2013.08.013

Title

Pharmacokinetics, brain distribution and plasma protein binding of carbamazepine and nine derivatives: new set of data for predictive *in silico* ADME models

Author names and affiliations

Ana Fortuna[1,2], Gilberto Alves[2,3*], Patrício Soares-da-Silva[4,5], Amílcar Falcão[1,2]

[1] Department of Pharmacology, Faculty of Pharmacy, University of Coimbra, Pólo das Ciências da Saúde, Azinhaga de Santa Comba, 3000-548 Coimbra, Portugal

[2] CNC – Centre for Neuroscience and Cell Biology, University of Coimbra, 3004-517 Coimbra, Portugal

[3] CICS-UBI – Health Sciences Research Centre, University of Beira Interior, Av. Infante D. Henrique, 6200-506 Covilhã, Portugal

[4] Department of Research and Development, BIAL, Av. da Siderurgia Nacional, 4745-457 S. Mamede do Coronado, Portugal

[5] Department of Pharmacology and Therapeutics, Faculty of Medicine, University of Porto, 4200-319 Porto, Portugal

*** Corresponding author**

Gilberto Alves, PharmD, PhD

Faculty of Health Sciences, University of Beira Interior

CICS-UBI – Health Sciences Research Centre, University of Beira Interior

Av. Infante D. Henrique, 6200-506 Covilhã, Portugal

Phone: +351 275329002 / Fax: +351 275329099

E-mail address: gilberto@fcsaude.ubi.pt

Abstract

In silico approaches to predict absorption, distribution, metabolism and excretion (ADME) of new drug candidates are gaining a relevant importance in drug discovery programs. When considering particularly the pharmacokinetics during the development of oral antiepileptic drugs (AEDs), one of the most prominent goals is designing compounds with good bioavailability and brain penetration. Thus, it is expected that *in silico* models able to predict these features may be applied during the early stages of AEDs discovery. The present investigation was mainly carried out in order to generate *in vivo* pharmacokinetic data that can be utilized for development and validation of *in silico* models.

For this purpose, a single dose of each compound (1.4 mmol/kg) was orally administered to male CD-1 mice. After quantifying the parent compound and main metabolites in plasma and brain up to 12 h post-dosing, a non-compartmental pharmacokinetic analysis was performed and the corresponding brain/plasma ratios were calculated. Moreover the plasma protein binding was estimated *in vitro* applying the ultrafiltration procedure.

The present *in vivo* pharmacokinetic characterization of the test compounds and corresponding metabolites demonstrated that the metabolism extensively compromised the *in vivo* activity of CBZ derivatives and their toxicity. Furthermore, it was clearly evidenced that the time to reach maximum peak concentration, bioavailability (given by the area under the curve) and metabolic stability (given by the $AUC_{0\text{-}12h}$ ratio of the parent compound and total systemic drug) influenced the *in vivo* pharmacological activities and must be considered as primary parameters to be investigated. All the test compounds presented brain/plasma ratios lower than 1.0, suggesting that the blood-brain barrier restricts drug entry into the brain. In agreement with *in vitro* studies already performed within our research group, CBZ, CBZ-10,11-epoxide and oxcarbazepine exhibited the highest brain/plasma ratios (> 0.50), followed by eslicarbazepine, *R*-licarbazepine, *trans*-diol and BIA 2-024 (ratios within 0.05-0.50). BIA 2-265 was not found in the biophase, probably due to its high plasma-protein bound fraction (> 90%) herein revealed for the first time.

The comparative *in vivo* pharmacokinetic data obtained in the present work might be usefully applied in the context of discovery of new antiepileptic drugs that are derivatives of CBZ.

Keywords: Antiepileptic drugs; Carbamazepine; Pharmacokinetics; *In silico*; Brain; Plasma protein binding.

Abbreviations: ADME, absorption, distribution, metabolism and excretion; AEDs, antiepileptic drugs; AUC, area under the plasma drug concentration-time curve; BBB, blood-brain barrier; CBZ, carbamazepine; CBZ-E, carbamazepine-10,11-epoxide; C_{max}, maximum peak concentration; CNS, central nervous system; DMSO, dimethyl sulfoxide; ED_{50}, effective dose for protecting at 50%; ESL, eslicarbazepine acetate; HPLC, high performance liquid chromatography; IS, internal standard; LOQ, limit of quantification; MES, maximal electroshock seizure; MRT, mean residence time; NSB, non-specific binding; OXC, oxcarbazepine; PPB, plasma protein binding; *R*-Lic, *R*-licarbazepine; *S*-Lic, eslicarbazepine; TD_{50}, lowest median toxic dose at 50%; t_{max}, time to reach maximum peak concentration; $t_{1/2}$, apparent terminal elimination half-life; *trans*-diol, 10,11-*trans*-dihydroxy-10,11-dihydro-carbamazepine; UF, ultrafiltration.

1. Introduction

Epilepsy is a chronic neurological disorder that affects around 50 million people worldwide (Nei and Heys, 2010). Since the clinical introduction of the first antiepileptic drug (AED) appreciable efforts have been carried out in order to improve the quality of life of the patients. Today, a wide therapeutic range of AEDs with various activity spectra and tolerability profiles is available (Bialer, 2012a). Nevertheless, the truth is that the new AEDs developed so far are not completely effective since only 70% of the epileptic patients become seizure free when administered with one of those drugs. In opposition, the remaining 30% of the patients often develop a chronic form of epilepsy that is refractory to several pharmacological treatments (Brodie, 2005; Luszczki, 2009). Thus, the discovery of new AEDs still remains a ceaseless challenge for the medicinal chemistry and pharmacology (Bialer and White, 2010; Mackey, 2010; Schmidt 2010, 2011).

One of the techniques that has become commonplace for searching novel AEDs is based on chemical and/or structural modifications of currently available AEDs, in order to obtain more effective drugs with better pharmacokinetic properties than the available maternal AED (Rogawski, 2006; Bialer, 2010; Bialer and White 2010; Bialer 2012). As recently emphasized by Bialer (2012a), pharmacokinetic-based design of AEDs has been carried out to enhance the absorption, plasma exposure and brain penetration of the active entity and/or circumvent the formation of toxic metabolites. Bearing this in mind and the fact that almost 40% of the drug candidates fail during preclinical phases due to their inadequate pharmacokinetic properties (Yengi et al., 2007), rational design approaches should be applied early in drug discovery programs. The current high pressure to successfully develop new drugs is implying fast *in silico* and *in vitro* methodologies with the purpose of optimizing those particular pharmacokinetic properties of the prototypes (Hosea and Jones, 2013). The *in silico* approach intends to simulate and predict the absorption, distribution, metabolism and excretion (ADME) properties of compounds, and it has gained an increase importance in the recent years. However these methodologies must be firstly validated and conjugated with *in vivo* results in order to adequately foresee the *in vivo* pharmacokinetics. Up to date, the information regarding the *in vivo* pharmacokinetic parameters of several derivatives of current AEDs is scarce and, when available, it results from distinct protocols, hampering data integration.

Thus, in an attempt to support and validate *in silico* pharmacokinetic-based drug design of novel and chemically related AEDs, this work was planned to acquire new *in vivo* data considering the systemic exposure, biodisposition and brain penetration of carbamazepine (CBZ) and nine derivatives after oral administration to mice. These *in vivo* pharmacokinetic data can also be incorporated in more complete and complex *in silico* models (Margineanu, 2012) in order to select those compounds that influence *in vitro* targets at appropriate concentrations and

simultaneously exhibit acceptable bioavailability and brain penetration instead of selecting the candidate that best sticks only the pharmacodynamic target or the pharmacokinetic characteristics. The set of test compounds included not only clinically available drugs such as CBZ, oxcarbazepine (OXC) and eslicarbazepine acetate (ESL), but also *S*-licarbazepine (*S*-Lic), *R*-licarbazepine (*R*-Lic), carbamazepine-10,11-epoxide (CBZ-E), 10,11-*trans*-dihydroxy-10,11-dihydro-carbamazepine (*trans*-diol), BIA 2-024, BIA 2-059 and BIA 2-265. As shown in Figure 1, all the compounds share the dibenz[*b,f*]azepine-5-carboxamide group. Furthermore, due to its influence on pharmacokinetics and pharmacodynamics, the plasma protein binding percentage was also determined for all the test compounds applying an *in vitro* methodology.

2. Material and Methods

2.1. Chemicals and reagents

OXC, ESL, CBZ-E, *S*-Lic, *R*-Lic, *trans*-diol, BIA 2-059, BIA 2-024 and BIA 2-265 were kindly supplied by BIAL (Porto, Portugal). CBZ, chloramphenicol and 10,11-dihydrocarbamazepine were purchased from Sigma-Aldrich (St Louis, MO, USA).

High performance liquid chromatography (HPLC) gradient grade methanol and acetonitrile were purchased respectively from Fisher Scientific (Leicestershire, UK) and Lab-Scan (Sowinskiego, Poland). Ultrapure water (HPLC grade, >15 MΩ) was obtained by means of a Milli-Q water apparatus from Millipore (Milford, MA, USA). Ethyl acetate, sodium dihydrogen phosphate dihydrate, di-sodium hydrogen phosphate dehydrate, sodium chloride, potassium dihydrogen phosphate and hydrochloric acid 37% were purchased from Merck KGaA (Darmstadt, Germany). Carboxymethylcellulose sodium salt for preparation of drug suspensions was obtained from Sigma (St. Louis, USA).

2.2. *In vivo* pharmacokinetic studies

2.2.1. Animals and experimental design

Adult male CD-1 mice were purchased from Harlan™ (Udin, Italy) and were approximately 25-35 g at the time of the study. The animals were housed for at least one week in local facilities under climate- and light-controlled environmental conditions (22±1 ºC, 50±5% humidity, 12 h light/dark cycle) until performing the experiments. Mice were freely fed with a regular standard chow diet (4RF21, Mucedola, Italy) and provided with tap water *ad libitum* before and immediately after drug administration. All experimental protocols involving the use of animals were conducted in accordance with the European Directive (86/609/EEC) for the accommodation and care of laboratory animals and approved by the Portuguese Veterinary General Division.CBZ, OXC, ESL, CBZ-E, *S*-Lic, *R*-Lic, *trans*-diol, BIA 2-059, BIA 2-024 and BIA 2-265 were dissolved in dimethyl sulfoxide (DMSO) and then suspended in a 0.5%

carboxymethylcellulose aqueous solution (the maximum quantity of DMSO in the final suspension was 5%). A single dose (1.4 mmol/kg) of each compound was administered by oral gavage (25 mL/kg) to groups of mice. Prior to sample collection, mice were sacrificed by cervical dislocation and decapitation at 0.25, 0.5, 1, 2, 4, 8 and 12 h post-dosing. Samples were collected from four mice at each time point. Blood samples were immediately collected to heparinised tubes and centrifuged at 4000 rpm for 10 min at 4 ºC. Plasma supernatant was frozen at -30 ºC until analysis. After exsanguination, the brain was quickly excised, weighted and homogenised in a 0.1 M sodium phosphate buffer pH 5 (4 mL of buffer per g of tissue) using a THOMAS® teflon pestle tissue homogenizer. The homogenates were centrifuged at 4800 rpm for 15 min at 4 ºC, originating supernatants that were also stored at -30 ºC until analysis.

2.2.2. Sample pre-treatment

Samples of mice plasma and brain homogenate were processed by a solid-phase extraction procedure based on methods previously published (Fortuna et al., 2011a, 2011b). An aliquot of plasma sample (300 µL) was added to 700 µL of 0.1 M sodium phosphate buffer (pH 5) and spiked with the adequate internal standard (IS) working solution, while each sample of brain homogenate supernatant (1 mL) was only spiked with IS. Samples were vortex-mixed and loaded into Oasis® HLB cartridges (30 mg, 1 mL, Waters, Milford, MA, USA), previously conditioned with 1 mL of methanol, 1 mL of acetonitrile and 1 mL of water-acetonitrile (95:5, v/v). After sample elution, the loaded cartridges were submitted to -40 kPa and washed four times with 1 mL of water-methanol (90:10, v/v). After drying the sorbent, the analytes were eluted with 1 mL of ethyl acetate under a gentle vacuum. The eluates were evaporated to dryness under a nitrogen stream at 45 °C and the residues were reconstituted in 100 µL of HPLC mobile phase, transferred to a 0.22 µm Spin-X centrifugal filter and centrifuged at 13400 rpm for 2 min. Lastly 20 µL of the final filtered samples were injected into the HPLC system.

2.2.3. Quantification of CBZ and derivatives in plasma and brain tissue

A BAS-480 liquid chromatography system equipped with a PM-80 pump, a Rheodyne manual injector with a 20 µL loop, a BAS UV-116 UV-Vis detector, a BAS LC-22C temperature controller, a BAS DA-5 chromatography control and a data system interface (all from Bioanalytical Systems, West Lafayette, IN, USA) was used for all analysis. Data collection and integration were achieved by means of the BAS Chromgraph Control and Chromgraph Report software version 2.30.

The quantification of CBZ, OXC, ESL, *S*-Lic, *R*-Lic and CBZ-E after their administration to mice was carried out at 40 ºC, on the chiral column LiChroCART 250-4 ChiraDex, using a

mobile phase of water and methanol (88:12, v/v) pumped at 0.9 mL/min and an UV detector set at 235 nm. Chloramphenicol was used as IS. The limits of quantification (LOQ) of CBZ, OXC, ESL, *S*-Lic, *R*-Lic and CBZ-E were respectively 0.4, 0.1, 0.2, 0.2, 0.2 and 0.2 µg/mL in plasma and 0.12, 0.06, 0.06, 0.06, 0.06 and 0.12 µg/mL in the supernatant of brain homogenate (Fortuna et al., 2011a). Similar conditions were used for the quantification of BIA 2-059, BIA 2-024, BIA 2-265 and their main metabolites (OXC, *S*-Lic, *R*-Lic). Separation was carried at 35 ºC, with a mobile phase of water-methanol (92:8, v/v) pumped at 0.7 mL/min and using CBZ-E as IS; the LOQ was defined as 0.2 µg/mL and 0.06 µg/mL for all analytes in plasma and brain homogenate, respectively (Fortuna et al., 2011b). The quantification of *trans*-diol in mice plasma and brain homogenate after its administration to the animals was attained by an achiral HPLC-UV method, adapted from another previously developed and validated technique (Fortuna et al., 2011a), using water-methanol-acetonitrile (64:30:6, v/v/v), at a flow rate of 1 mL/min and a C_{18}-reversed-phase column LiChroCART® Purospher® Star (Merck KGaA, Darmstadt, Germany). The 10,11-dihydrocarbamazepine was used as IS. The calibration range of *trans*-diol in the plasma and brain of mice were respectively 0.2–10 µg/mL and 0.06–0.30 µg/mL ($r^2 \geq 0.998$).

At LOQ levels, the precision (expressed as percentage of coefficient of variation) and accuracy (expressed by the deviation from nominal value in percentage) were, respectively, 13.6% and -1.25% in plasma and 2.7% and 15.2% in brain homogenate supernatants. The overall intra and inter-day precision was less than 9.50% and the intra and inter-day accuracy ranged from -11.19 to 1.86%.

2.2.4. Pharmacokinetic data analysis

The maximum peak concentration (C_{max}) of the dibenz[*b*,*f*]azepine-5-carboxamide derivatives in plasma and brain tissue and the time to reach C_{max} (t_{max}) were determined directly from the measured concentration values. The other pharmacokinetic parameters were estimated from mean concentration data ($n = 4$) obtained at each time point (0.25, 0.5, 1, 2, 4, 8 and 12 h post-dosing) by a non-compartmental analysis using the WinNonlin version 4.1 (Pharsight Co, Mountain View, CA, USA): AUC from time zero to the last sampling time (12 h) at which concentrations were at or above the LOQ ($AUC_{0–12h}$) was calculated using the linear trapezoidal rule; AUC from time zero to infinity ($AUC_{0–\infty}$) was calculated from $AUC_{0–12h} + (C_{last}/\lambda_z)$, where C_{last} is the last quantifiable concentration and λ_z is the apparent terminal rate constant, calculated by log-linear regression of the terminal segment of the concentration–time profile; and lastly, the apparent terminal elimination half-life ($t_{1/2}$) and mean residence time (MRT). Mean plasma and tissue concentrations lower than the LOQ of the assay were taken as zero for all calculations.

In order to assess the extent of distribution of each compound to the brain, brain-to-plasma ratios were calculated considering C_{max}, $AUC_{0\text{-}12h}$ and $AUC_{0\text{-}\infty}$.

2.3. *In vitro* determination of plasma protein binding

The binding of the dibenz[*b*,*f*]azepine-5-carboxamide derivatives to mice plasma proteins was investigated *in vitro* by ultrafiltration (UF) experiments using a Microcon® Ultracel YM-30 device with a cellulose membrane filter of 0.32 cm^2 and 30 kDa cut-offs (Millipore, Bedford, USA). The studies were performed at 40 µM for CBZ, 8 µM for OXC, 4 µM for CBZ-E, 100 µM for BIA 2-024 and BIA 2-265, 15 µM for *trans*-diol and 6 µM for ESL and BIA 2-059. Stock solutions of each compound were prepared in DMSO and thereafter accurately diluted in Sorënsen buffer (pH 7.4) in order to obtain the correspondent spiking solution used in the assay.

Plasma aliquots of 1 mL (n = 4) were spiked with the correspondent quantity of drug and then incubated in a water bath under circular shake at a rate of 10 rpm, for 30 min, at 37 ºC. Following incubation, 300 µL of plasma were used for the determination of the total concentration of each test compound and 500 µL were transferred to the Microcon® Ultracel YM-30 UF device, sealed with the attached cap and centrifuged at 14000 rpm, 37 ºC, during 30 min. Afterwards, the concentration of the compound was determined in 300 µL of the ultrafiltrate, in order to obtain the unbound drug concentration. The analysis of these samples was performed by adapting the HPLC techniques described in section 2.2.3.

The PPB (%) obtained by UF was calculated considering the equation (1) stated by Fukushima et al. (2009):

$$PPB = \frac{C_t - C_f}{C_t} \times 100$$

where C_t corresponds to the total concentration in spiked plasma without having been subjected to UF and C_f represents the free drug concentration obtained in the ultrafiltrates.

The non-specific binding (NSB) of each test compound to the filter membrane and plastic parts of the UF apparatus was assessed using spiked isotonic Sorënsen phosphate buffer instead of using spiked plasma. The NSB (%) was estimated according to the equation (2):

$$NSB = \frac{C_{tb} - C_{fb}}{C_{tb}} \times 100$$

where C_{tb} refers to the total compound concentration in the spiked buffer without UF and C_{fb} is the free drug concentration obtained in the corresponding filtrate after UF.

2.4. Correlation between pharmacokinetic parameters, physicochemical characteristics and PPB

The degree of association between the principal pharmacokinetic parameters (C_{max}, AUC_{0-12h} and brain-to-plasma ratios) and molecular mass (MM), pKa, octanol-water partition coefficient (LogP), polar surface area (PSA) and PPB of drug candidates was investigated applying GraphPad Prism version 5.00 for Microsoft Windows (GraphPad Software, USA) to determine the Pearson's correlation coefficient (r) and a minimum p value of 0.05 was used as a significance level for the tests.

3. Results

3.1. Plasma disposition of CBZ and its derivatives

The plasma concentration-time profiles of the ten test compounds and respective main metabolites following their oral administration to mice are plotted in Figure 2 and the corresponding pharmacokinetic parameters estimated by non-compartmental analysis are summarized in Table 1. In particular situations, the pharmacokinetic parameters could not be calculated because the compound was not detected in the sample or because it appeared below the LOQ of the analytical technique. Taking into account the t_{max} values reported in Table 1, it is evident that almost all the parent compounds reached the maximum peak plasma concentration until 1 h after oral administration, suggesting that the dibenz[*b,f*]azepine-5-carboxamide derivatives are rapidly absorbed through the gastrointestinal tract. BIA 2-024 was the only exception as it presented a t_{max} of approximately 2 h and, therefore, it is regarded as the compound most slowly absorbed.

From the direct analysis of the profiles depicted in Figure 2, it is clearly observed that CBZ-E, *trans*-diol and BIA 2-265 did not originate any other compound for which the bioanalytical techniques had been developed. In fact, no additional peaks appeared in the chromatograms beyond those that corresponded to the administered compound or IS. Among the other seven derivatives, BIA 2-024 was the less metabolized compound, exhibiting an AUC_{0-12h} that corresponded to approximately 98.6% of the total drug exposure in plasma. Indeed, BIA 2-024 originated *R*-Lic and *S*-Lic in a very small extent (< 2%), suggesting that the parent compound is considerably stable from the metabolic viewpoint and probably the main responsible for its anticonvulsant action. Like BIA 2-024, *R*-Lic, *S*-Lic and OXC also demonstrated to be very stable in mice, being present as 88.0%, 82.9% and 82.7% of the total systemic drug exposure (as assessed by AUC_{0-12h}).

It is interesting to highlight the difference found between *R*-Lic and *S*-Lic; while *S*-Lic mainly originated OXC, *R*-Lic was metabolised in a lower extent than *S*-Lic, originating not only OXC but also measurable amounts of the eutomer (*S*-Lic). Plasma concentrations of BIA 2-024, *R*-Lic, *S*-Lic and OXC declined with a $t_{1/2}$ of respectively 3.47, 2.43, 7.66 and 8.99 h. MRT for BIA 2-024, *R*-Lic, *S*-Lic and OXC were 5.28, 3.56, 10.22 and 12.77 h, respectively. Therefore,

although the compounds can be considered metabolically stable, their distinct $t_{1/2}$ and MRT values clearly support the view that *S*-Lic and OXC remain unchanged in plasma for a time period significantly longer than *R*-Lic or BIA 2-024.

In opposition, CBZ, ESL and BIA 2-059 were the most extensively metabolized in mice. CBZ mainly originated CBZ-E considering the high C_{max} and $AUC_{0\text{-}12h}$ values reported for this metabolite after the administration of CBZ. Although other minor compounds were detected by the analytical method, they were not identified or quantified since the method was not validated for that purpose. Thus, and considering only the production of CBZ-E, both the parent compound and its main metabolite presented similar total drug exposure in plasma (approximately 50%). According to Table 1, the distinct values of $t_{1/2}$ of CBZ-E after its administration and the administration of CBZ (4.89 h *versus* 12.52 h) are obvious, and the same is observed regarding the MRT values (7.93 h *versus* 19.73 h). This probably results from the fact that, as a metabolite, CBZ-E is simultaneously produced and subjected to elimination processes while after its own administration, CBZ-E becomes immediately available in plasma presenting a t_{max} value of 0.5 h and remaining less time in the body.

Analyzing BIA 2-059, it appears as the only parent compound that, when detected in plasma samples, exists at concentrations below the LOQ of the method (0.2 μg/mL). As depicted in Figure 2, BIA 2-059 was rapidly metabolized to *R*-Lic, *S*-Lic and OXC which corresponded respectively to 88.8%, 1.0% and 10.2% of the total systemic drug exposure (as assessed by $AUC_{0\text{-}12h}$) (Table 1). However, when comparing BIA 2-059 with its enantiomer (ESL), a distinct pharmacokinetic profile was found not only for the parent compounds but also for their metabolites. ESL was mainly biotransformed to *S*-Lic (82.9%) and to a minor extent to OXC (16.8%) and *R*-Lic (0.21%). It is important to highlight that the extension of systemic exposure to *S*-Lic, *R*-Lic and OXC (assessed by $AUC_{0\text{-}12h}$) were, respectively, 2.2%, 88.0% and 9.7% after the *R*-Lic administration, while the systemic exposure to *S*-Lic and OXC was respectively 82.9% and 17.1% after *S*-Lic administration (Table 1). These values are similar to those described after the administration of ESL and BIA 2-059, supporting the view that each one of the acetate derivatives (ESL and BIA 2-059) is considered a prodrug of the corresponding alcohol compound.

3.2. Brain disposition and blood–brain distribution of CBZ and its derivatives

As the brain is the target organ of the AEDs, concentrations of the dibenz[*b*,*f*]azepine-5-carboxamide derivatives and main metabolites were also determined in mice brain homogenate after single oral administration of each compound at 1.4 mmol/kg. Figure 3 shows the mean brain concentration-time profiles of the various compounds and respective metabolites while the corresponding pharmacokinetic parameters are summarized in Table 2.

Globally analyzing the brain concentration-time profiles, the t_{max} of several compounds was slightly displaced to the right in comparison to those observed in plasma. The exceptions included ESL, CBZ-E, OXC and BIA 2-024 that show, in both matrices, t_{max} values of 0.5 h, 0.5 h, 1 h and 2 h, respectively. Similar findings were observed considering the t_{max} values of the metabolites (Table 2). This may indicate that ESL, CBZ-E, OXC and BIA 2-024 cross the blood-brain barrier (BBB) more promptly than the remaining derivatives.

Similarly to the analysis aforementioned in the previous section regarding the metabolic stability of the compounds, the results presented in Table 2 demonstrated that OXC and BIA 2-024 still remained considerably stable in the brain accounting respectively for 96.26% and 90.10% of the total brain drug exposure. Moreover, the other compounds also demonstrated similar metabolic stability in the brain to that observed at systemic level.

It was also clear that the test compounds presented lower values of C_{max}, $AUC_{0\text{-}12h}$ and $AUC_{0\text{-}\infty}$ in the brain than in plasma (Figure 3, Table 2). In order to assess the extent of distribution of each compound to the target organ, C_{max}, $AUC_{0\text{-}12}$ and $AUC_{0\text{-}\infty}$ brain/plasma ratios were calculated (Table 3). None of these ratios could be calculated for BIA 2-059, for *R*-Lic after administration of *S*-Lic and for *S*-Lic after BIA 2-024 administration, because their plasma levels were below the LOQ of the bioanalytical methods. Some values of $AUC_{0\text{-}12h}$ and $AUC_{0\text{-}\infty}$ brain/plasma ratios could not be calculated due to the fact that their AUC values in brain were not possible to calculate. All the values of brain/plasma ratios calculated considering C_{max} and $AUC_{0\text{-}12h}$ were lower than 1.0 (Table 3), suggesting that the BBB restricts drug entry into the brain. Taking into account the ratios assessed by both pharmacokinetic parameters depicted in Table 3, three groups of compounds could be distinguished. One is constituted by compounds with C_{max} and $AUC_{0\text{-}12}$ ratios higher than 0.50 and includes OXC, CBZ, CBZ-E. Another group is characterized by at least one of the ratios values between 0.05 and 0.50 and includes *S*-Lic, *R*-Lic, *trans*-diol and BIA 2-024. Finally, there is BIA 2-265 for which the ratios are lower than 0.05.

3.3. Plasma protein binding of CBZ and its derivatives

The concentration used for measuring the PPB of each test compound was defined according to previous studies and included the therapeutic range of compounds (Fortuna et al., 2010, 2012b). Once no saturation phenomenon was observed (Fortuna et al., 2012a) and, regarding that for ethical reasons in the present work we should only investigate one concentration, the middle concentration was chosen for each compound.

The NSB percentage of the ten dibenz[*b,f*]azepine-5-carboxamide derivatives to the UF device was lower than 5%. This result is considered negligible and, hence, no correction factor was applied to calculate the PPB by UF.

The percentage of PPB found for each compound under *in vitro* conditions is depicted in Table 4. BIA 2-265 is the compound with the highest value of PPB (almost 90%) while *trans*-diol is the one with the lowest value (approximately 23%). The other compounds present intermediate values, but CBZ and OXC should be highlighted, as their percentages of PPB were the highest (71.61% and 76.56%, respectively).

3.4. Correlation between pharmacokinetic parameters, physicochemical characteristics and PPB

The physicochemical properties of the ten compounds herein under investigation are depicted in Table 5. There was no correlation between plasmatic C_{max} or $AUC_{0\text{-}12h}$ with any physicochemical characteristic under study (MM, pKa, logP and PSA). However, the percentage of PPB did exhibit a significant correlation with C_{max} (r = - 0.900, p = 0.002) and $AUC_{0\text{-}12h}$ (r = -0.731, p = 0.039). In opposition, no correlation was found between brain pharmacokinetic parameters and PPB. Surprisingly, when considering C_{max} or $AUC_{0\text{-}12h}$ values obtained in brain tissue, a good correlation was obtained only with PSA (r = -0.850, p = 0.007 for C_{max} and r = -0.834, p = 0.01 for $AUC_{0\text{-}12h}$). As far as the $AUC_{0\text{-}12h}$ brain/plasma ratios were concerned, a significant correlation with MM (r = -0.799, p = 0.017) and PSA (r = -0.872, p = 0.005) was observed and, similarly, C_{max} was also well correlated with MM (r = -0.700, p = 0.049) and PSA (r = -0.796, p = 0.018). However no correlations were found between $AUC_{0\text{-}12h}$ or C_{max} ratios when compared to logP, pKa or PPB.

4. Discussion

Therapeutic targets located within the brain represent unique challenges for drug discovery programs. Because of the tight endothelial junctions and efflux transporters expressed in the BBB, a common defiance encountered in oral AEDs discovery is the conversion of a potent compound with *in vitro* activity into a compound that reaches considerable levels in circulation and brain tissue, avoiding the lack of *in vivo* activity usually attributed to suboptimal pharmacokinetic characteristics (Partridge, 2003).

Thus, the main purpose of this study was to report the pharmacokinetics of ten derivatives of CBZ after their oral administration to mice and determine their systemic bioavailability, brain/plasma partition ratio and PPB in order to evaluate whether the pharmacological differences between the ten derivatives of CBZ may be a consequence of their distinct systemic exposure and/or plasma-to-brain distribution. Simultaneously this data may be useful for supporting *in silico* models.

This is the first time that a wide set of dibenz[*b*,*f*]azepine-5-carboxamide derivatives is studied for a systemic and brain *in vivo* pharmacokinetic evaluation after oral administration to mice.

Mouse was the specie herein chosen because rodents are generally used as a reference predictive animal model to evaluate the pharmacodynamics of drug candidates during the discovery of new AEDs applying the maximal electroshock seizure (MES) test (Castel-Branco et al., 2009). In addition, mice were preferred in relation to rats based on *in vivo* and *in vitro* investigations which have revealed that the metabolism of ESL, CBZ, and BIA 2-024 in humans is more similar to that observed in mice than in rats (Hainzl et al., 2001; Hidaka et al., 2005; Alves et al., 2008a, 2008b). The single dose of 1.4 mmol/kg was chosen based on the fact that previous studies have revealed that this dose was associated with no significant toxicity and provided a systemic exposure to the active metabolite of OXC and ESL (*S*-Lic) comparable with those occurring in epileptic patients after treatment with therapeutic doses of OXC (González-Esquivel et al., 2000) and ESL (Bialer et al., 2004). As the present research investigation intended to compare all the ten derivatives, an equimolar dose was maintained for the remaining compounds. Toxicity was not herein investigated because it falls outside the scope of the present work, however it must be emphasized that no animal died throughout the pharmacokinetic studies. The animals particularly administered with CBZ, OXC, ESL, *S*-Lic and BIA 2-024 were more sleepy and apathetic and only few animals administered with CBZ and CBZ-E showed some motor impairments which tended to disappear after 1 h post-dosing.

The analysis of the pharmacokinetic profiles herein carried out for the ten dibenz[*b*,*f*]azepine-5-carboxamide derivatives, clearly demonstrated that all of them were quickly absorbed from the mice gastrointestinal tract, except BIA 2-024. This particular compound presents an oxime moiety in 10^{th} position and reaches C_{max} only 2 h after its administration, probably because it is slowly absorbed through the intestinal membrane. Interestingly, among all the derivatives, BIA 2-024 was the one that presented the lowest value of *in vitro* apparent permeability through mice intestine and the highest efflux ratio that is associated to its high affinity to the P-glycoprotein (Fortuna et al., 2012b). These observations may hamper its oral absorption, contributing to the higher t_{max} found for BIA 2-024 in comparison to the other test compounds. Furthermore, together with the high metabolic stability herein observed for BIA 2-024, they may also explain the high value of its $AUC_{0\text{-}12h}$ despite the slow intestinal absorption. These results are in agreement with other *in vivo* studies, as well as, with *in vitro* investigations performed in human liver microsomes (Hainzl et al., 2002)

Due to its impact on the efficacy and safety of new chemical entities, metabolic stability should be early investigated to select and/or design AEDs. The metabolic stability herein is given by the $AUC_{0\text{-}12h}$ ratio of the parent compound and the total systemic drug. Compounds poorly metabolized (e.g., BIA 2-024) originated high values of systemic drug exposure, which may allow larger intervals between administrations at the steady-state conditions. In opposition,

compounds extensively metabolized may originate high quantities of toxic derivatives and diminish the therapeutic index of the parent compound. For instance, CBZ, which is well known for its considerable neurological and motor toxicity in humans ascribed to the metabolite CBZ-E (Myllynen et al., 2002; Spina, 2002), presented the lowest value of effective dose for protecting 50% of the rats (ED_{50}) against MES-induced seizures and the lowest median toxic dose (TD_{50}) in the rotarod test (Ambrósio et al., 2002; Benes et al., 1999; Bonifácio et al., 2001). This means that, at lower concentrations, CBZ develops motor impairment that is not observed for the other compounds and its protective index (given by the ratio between ED_{50} and TD_{50}) is considerably lower in relation to OXC, ESL, *S*-Lic, *R*-Lic, BIA 2-059 and BIA 2-024 (Benes et al., 1999; Bonifácio et al., 2001; Learmonth et al., 2001). These *in vivo* pharmacodynamic behaviours are strongly supported by our results which revealed that CBZ was the only dibenz[*b,f*]azepine-5-carboxamide derivative extensively metabolized to CBZ-E. This is evidenced by the high values of $AUC_{0\text{-}12h}$, $t_{1/2}$ and MRT of CBZ-E in plasma and brain after CBZ administration, favouring the accumulation of the metabolite in brain for such a long time that may induce the remarkable toxicity observed *in vivo*.

On the other hand, *in vivo*, OXC showed a higher protective index than CBZ in spite of its higher toxicity observed *in vitro* (Araújo et al., 2004). This apparent discrepancy might be explained by the fact that, *in vivo*, OXC has yielded a metabolite (*S*-Lic) that is more innocuous than the major metabolite of CBZ. However, the protection conferred by OXC against MES-induced seizures in rats is lower than that obtained after ESL administration (Benes et al., 1999). Considering the results reported herein, this may be due to the fact that ESL is rapidly and extensively metabolized to *S*-Lic, which bioavailability measured in terms of $AUC_{0\text{-}12h}$ was approximately 6 times greater than that obtained after oral intake of an equimolar dose of OXC (Table 2).

The metabolism also has impact when considering two dibenz[*b,f*]azepine-5-carboxamide derivatives that are enantiomers (ESL and BIA 2-059). The bioavailability of *S*-Lic after oral administration of BIA 2-059 to mice was significantly lower than that obtained after ESL or OXC administration. Interestingly, this finding may explain the considerable lower protective index of BIA 2-059 against MES-induced seizures in rats, compared to that of ESL, in spite of their *in vitro* similar ability to inhibit the sodium uptake into cortical synaptosomes (Benes et al., 1999; Hainzl et al., 2001).

All the aforementioned findings clearly sustain that the t_{max}, bioavailability (given by $AUC_{0\text{-}12h}$) and metabolic stability of dibenz[*b,f*]azepine-5-carboxamide derivatives must be considered primary parameters to be investigated in parallel with *in vitro* and *in vivo* pharmacodynamics because they clearly determined the pharmacological activity *in vivo*.

Additionally, when the targeted site of action lies within the CNS, the BBB represents a relevant barrier for the access of compounds to the target organ and it is frequently responsible for the relatively low success rate in discovery and development of CNS drugs (Partridge, 2005). For instance, *in vitro* it was demonstrated that BIA 2-024 had a higher potency to bind to sodium channels and modulate sodium entry than CBZ. However, *in vivo*, it is as effective as CBZ and OXC at controlling seizures (Ambrósio et al., 2001; 2002; Benes et al., 1999; Learmonth et al., 2001). Although this may seem contradictory, the low brain-to-plasma ratios herein obtained for BIA 2-024 in relation to those obtained for CBZ and the slower absorption of BIA 2-024 may justify its potency *in vivo*.

The stereoselective brain disposition of *S*-Lic and *R*-Lic is also noteworthy. As they are enantiomers, differing only in their spatial configuration (Figure 1) and in their ability to rotate plane-polarized light, it was expected that *S*-Lic and *R*-Lic would show similar $t_{1/2}$, C_{max} and $AUC_{0\text{-}12h}$ brain/plasma ratios. Nevertheless, the pharmacokinetic parameters obtained after *in vivo* administration of *S*-Lic or *R*-Lic to mice showed differences equal to or higher than 20% (Tables 2 and 3) and the brain/plasma ratios of *S*-Lic were approximately twice of those of *R*-Lic (0.25 *versus* 0.11 considering the C_{max} and 0.55 *versus* 0.26 considering the $AUC_{0\text{-}12h}$). These findings suggest a larger distribution of the eutomer (*S*-Lic) to the brain. Since the percentage of PPB of both enantiomers is similar (Table 4), it is highly probable that they have different affinities for multidrug efflux transporters at the BBB, including P-glycoprotein. Indeed, P-glycoprotein is normally expressed not only in the intestinal membrane but also on the luminal cell membrane of endothelial cells of BBB, reducing the brain disposition of drugs that interact with it (Fortuna et al., 2011c). Importantly, this transporter has been found to be over-expressed in endothelial cells, neurons and glial cells from human drug-resistance epileptic brain tissue, enhancing the extrusion of AEDs from brain to bloodstream and consequently lowering the brain concentration of several AEDs below effective (Aronica et al., 2012; Zhang et al., 2012). At this point, we have recently carried out *in vitro* studies to investigate the affinity of Lic enantiomers to P-glycoprotein and the results clearly revealed that *R*-Lic was likely to be transported by P-glycoprotein, in opposition to *S*-Lic (Fortuna et al., 2012b). Even though the experimental *in vivo* study herein described did not intend to analyse the P-glycoprotein influence on drug brain penetration, it is quite probable that the differences observed *in vivo* regarding the brain disposition of both enantiomers involve particularly this efflux transporter.

Considering the PPB obtained *in vitro* for the set of compounds herein under investigation, BIA 2-265 stands out as the only one that binds to plasma proteins in a percentage higher than 90%. Probably, the low unbound fraction of BIA 2-265 may have significantly contributed to the reduced brain disposition of the drug observed in vivo (Table 3). The remaining derivatives presented a wide range of PPB that varied from 23.02% to 76.56%. Unexpectedly, those with

higher brain exposure, including CBZ, OXC and CBZ-E, exhibited the highest values of PPB. This finding clearly demonstrates that the PPB of dibenz[*b,f*]azepine-5-carboxamide derivatives is not a major determinant of brain penetration, unless it is greater than 90%, such as for BIA 2-265.

The effect of molecular properties on the primary pharmacokinetic parameters (C_{max} and AUC_{0-12h}) and on the brain/plasma ratios was also herein considered. Particularly MM, logP, pKa and PSA were chosen not only because they are easily accessible but also because they represent major determinants of brain penetration of compounds (Partridge, 2005; Zhao et al., 2009). Generally, small, lipophilic, non-charged drugs diffuse more easily by passive transcellular mechanisms than the hydrophilic ones. In addition, only the free fraction of drug is available to cross the BBB (Lange et al., 2005) and a high lipophilicity also makes compounds more vulnerable to bind to plasma and efflux proteins (Perisic-Janjic et al., 2011). Based on the correlation analysis herein reported, it is important to emphasize that MM and PSA appeared to be the most important determinants of brain/plasma ratios and the AUC_{0-12h} and C_{max} values obtained in brain were also strongly correlated with PSA. Even though PPB did not correlated with brain-to-plasma ratios or pharmacokinetic profile in brain, it must be underlined that when it is higher than 90% (such in case of BIA 2-265) it may compromise brain penetration since only the plasmatic free fraction is available to cross the BBB and reach the target organ of AEDs.

In the *in vivo* pharmacokinetic evaluation herein performed, the relative systemic and brain exposure of CBZ and derivatives were, incontestably, linked to their pharmacodynamic and efficacy/toxicity readouts. Therefore, the sooner plasma and biophase pharmacokinetic information is obtained the less costly and risky is the discovery of AEDs. Moreover, it was demonstrated that PPB compromised the brain penetration of these compounds when higher than 90%; otherwise it had no influence. This would be very interesting to apply during the discovery phase of new AEDs derivatives of CBZ, as it would allow the development of compounds with higher probability of having adequate brain penetration. Nevertheless, it cannot be forgotten that, in parallel to this pharmacokinetic evaluation, additional tests in *in vivo* seizure-induced animal models must be performed in order to evaluate the drug efficacy, toxicity and protective effects.

Overall, it was evident that CBZ, CBZ-E and OXC presented the highest values of brain/plasma ratios and probably that fact sustains their pharmacological activity at the cerebral level. It is extremely interesting to point out that the *in vitro* methodologies previously developed within our research group (Fortuna et al., 2012a, 2012b) also demonstrated that CBZ, OXC and CBZ-E were the most permeable compounds though artificial and biological barriers, which is in agreement with the *in vivo* results herein presented.

5. Conclusions

The present *in vivo* studies clearly evidenced that the t_{max}, the extent of brain penetration and the metabolic stability of dibenz[*b*,*f*]azepine-5-carboxamide derivatives must be considered as primary parameters to be investigated in parallel with *in vitro* and *in vivo* pharmacodynamics because they clearly determine the *in vivo* activity. The comparative *in vivo* pharmacokinetic data obtained based on the protocol herein applied, together with those obtained through the *in vitro* approaches previously described by Fortuna et al (2012a, 2012b) and those of the *in vitro* and *in vivo* evaluation of efficacy and protective effects, may be useful for developing predictive *in silico* pharmacokinetic-based models that can be applied in the earlier stages of the discovery of new derivatives of CBZ.

Acknowledgments

This work was supported by Fundação para a Ciência e a Tecnologia (SFRH/BD/31390/2006), Portugal and by BIAL (Portela & C[a], S.A.), Portugal.

Conflicts of Interest

None of the authors has any conflict of interest to disclose.

References

Alves, G.; Figueiredo, I.; Falcão, A.; Castel-Branco, M.; Caramona, M.; Soares-da- Silva P. (2008a) Stereoselective disposition of S- and R-Licarbazepine in mice. *Chirality*, 20, 796-804.

Alves, G.; Figueiredo, I.; Castel-Branco, M.; Lourenço, N.; Falcão, A.; Caramona, M.; Soares-da-Silva, P. (2008b) Disposition of eslicarbazepine acetate in the mouse after oral administration. *Fundamental & Clinical Pharmacology*, 22, 529-536.

Ambrósio, A.F.; Silva, A.P.; Malva, J.O.; Soares-da-Silva, P.; Carvalho, A.P.; Carvalho, C.M. (2001) Inhibition of glutamate release by BIA 2-093 and BIA 2-024, two novel derivatives of carbamazepine, due to blockade of sodium but not calcium channels. *Biochemical Pharmacology*, 61, 1271-1275.

Ambrósio, A.F.; Soares-da-Silva, P.; Carvalho, C.M.; Carvalho A.P. (2002) Mechanisms of Action of Carbamazepine and Its Derivatives, Oxcarbazepine, BIA 2-093, and BIA 2-024. *Neurochemical Research*, 27, 121-130.

Araújo, I.M.; Ambrósio, A.F.; Leal, E.C., Verdasca, M.J.; Malva, J.O.; Soares-da-Silva, P.; Carvalho, A.P.; Carvalho, C.M. (2004) Neurotoxicity induced by antiepileptic drugs in cultured hippocampal neurons: a comparative study between carbamazepine, oxcarbazepine and two new putative antiepileptic drugs, BIA 2-024 and BIA 2-093. *Epilepsia*, 45, 1498-1505.

Benes, J.; Parada, A.; Figueiredo, A.A.; Alves, P.C.; Freitas, A.P.; Learmonth, D.A.; Cunha, R.A.; Garrett, J.; Soares-da-Silva, P. (1999) Anticonvulsant and Sodium Channel-Blocking Properties of Novel 10,11-Dihydro-5*H*-dibenz[*b*,*f*]azepine-5-carboxamide Derivatives. *Journal of Medicinal Chemistry*, 42, 2582-2587.

Bialer, M., White, H.S. (2010). Key factors in the discovery and development of new antiepileptic drugs. *Naure Reviews Drug Discovery*, 9, 68-82.

Bialer, M. (2012a). Chemical properties of antiepileptic drugs (AEDs). *Advanced drug delivery reviews*, 64, 887-895.

Bonifácio, M.J.; Sheridan, R.D.; Parada, A.; Cunha, R.A:; Patmore, L.; Soares-da-Silva. P. (2001) Interaction of the Novel Anticonvulsant, BIA 2-093, with Voltage-Gated Sodium Channels: Comparison with Carbamazepine. *Epilepsia*, 42, 600-608.

Brodie, M.J. (2005) Diagnosing and predicting refractory epilepsy. *Acta Neurologica Scandinavica, Supplementum,* 181, 36-39.

Castel-Branco, M.M.; Alves, G.L.; Figueiredo, I.V.; Falcão A.C.; Caramona, M.M. (2009) The maximal electroshock seizure (MES) model in the preclinical assessment of potential new antiepileptic drugs. *Methods & Findings in Experimental & Clinical Pharmacology*, 31, 101-106.

Hainzl, D.; Parada, A.; Soares-da-Silva, P. (2001) Metabolism of two new antiepileptic drugs and their principal metabolites S(+)- and R(-)-10,11-dihydro-10-hydroxy carbamazepine. *Epilepsy Research*, 44, 197-206.

Hainzl, D.; Loureiro, A.; Parada, A.; Soares-da-Silva, P. (2002) Metabolism of 10,11-dihydro-10-hydroxyimino-5H-dibenz/b,f/azepine-5-carboxamide, a potente antiepileptic drug. *Xenobiotica*, 32, 131-140.

Hidaka, M.; Okumura, M.; Fujita, K.; Ogikubo, T.; Yamasaki, K.; Iwakiri, T.; Setoguchi, N.; Arimori, K. (2005) Effects of pomegranate juice on human cytochrome P450 3A (CYP3A) and carbamazepine pharmacokinetics in rats. *Drug Metabolism and Disposition*, 33, 644-648.

Hosea, N.A.; Jones, H.M. (2013) Predicting pharmacokinetic profiles using *in silico* derived parameters. *Molecular Pharmaceutics*, dx.doi.org/10.1021/mp300482w

Fortuna, A.; Alves, G.; Soares-da-Silva, P.; Falcão, A. (2010) Binding of licarbazepine enantiomers to mouse and human plasma proteins. *Biopharmaceutics & Drug Disposition*, 31, 362-366.

Fortuna, A.; Bicker, J.; Alves, G.; Soares-da-Silva, P.; Falcão, A. (2011a) A chiral HPLC-UV method for the quantification of dibenz[b,f]azepine-5-carboxamide derivatives in mouse plasma and brain tissue: Eslicarbazepine acetate, carbamazepine and main metabolites. *Journal of Separation Science*, 34, 1391-1401.

Fortuna, A.; Alves, G.; Soares-da-Silva, P.; Falcão, A. (2011b) A chiral liquid chromatography method for the simultaneous determination of oxcarbazepine, eslicarbazepine, *R*-licarbazepine

and other new chemical derivatives BIA 2-024, BIA 2-059 and BIA 2-265, in mouse plasma and brain. *Biomedical Chromatography*, 26, 384-392.

Fortuna, A.; Alves, G.; Falcão, A. (2011c) In vitro and in vivo relevance of the p-glycoprotein probe substrates in drug discovery and development: focus on Rhodamine 123, Digoxin and Talinolol. *Journal of Bioequivalence & Bioavailability*, S2, doi:10.4172/jbb.S2-001.

Fortuna, A.; Alves, G.; Soares-da-Silva, P.; Falcão, A. (2012a) Optimization of a parallel artificial membrane permeability assay for the fast and simultaneous prediction of human intestinal absorption and plasma protein binding of drug candidates: application to dibenz[b,f]azepine-5-carboxamide derivatives. *Journal of Pharmaceutical Sciences*, 101, 530-540.

Fortuna, A.; Alves, G.; Soares-da-Silva, P.; Falcão, A. (2012b) Evaluation of the permeability and P-glycoprotein efflux of carbamazepine and several derivatives across mouse small intestine by the Ussing chamber technique. *Epilepsia*, 53, 529-538.

Fukushima, T.; Sone, Y.; Mitsuhashi, S.; Tomiya, M.; Toyo'oka, T. (2009) Alteration of kynurenic acid concentration in rat plasma following optically pure kynurenine administration: A Comparative Study between enantiomers. *Chirality* 21, 468-472.

Lange, E.C.M.; Ravenstijn, P.G.M.; Groenendaal, D.; Steeg T.J. (2005) Toward the prediction of CNS drug-effect profiles in physiological and pathological conditions using microdialysis and mechanism-based pharmacokinetic-pharmacodynamic modeling. *AAPS Journal*, 7, E532-E543.

Learmonth, D.A.; Benes, J.; Parada, A.; Hainzl, D.; Beliaev, A.; Bonifácio, M.J.; Matias, P.M.; Carrondo, M.A.; Garrett, J.; Soares-da-Silva, P. (2001) Synthesis, anticonvulsant properties and pharmacokinetic profile of novel 10,11-dihydro-10-oxo-5H-dibenz/b,f/azepine-5-carboxamide derivatives. *European Journal of Medicinal Chemistry*, 36, 227-236.

Luszczki, J.J. (2009) Third-generation antiepileptic drugs: mechanisms of action, pharmacokinetics and interactions. *Pharmacological Reports*, 61, 197-216.

Mackey, C. (2010) The anticonvulsants market *Naure Reviews Drug Discovery*, 9, 265-266.

Myllynen, P.; Pienimäki, P.; Raunio, H.; Vähäkangas, K. (1998) Microsomal metabolism of carbamazepine and oxcarbazepine in liver and placenta. *Human & Experimental Toxicology*, 17, 668-676.

Margineanu, D.G. (2012) Systems biology impact on antiepileptic drug discovery. *Epilepsy Research*, 98, 140-115.

Nei, M.; Hays, R. (2010) Sudden Unexpected Death in Epilepsy. *Current Neurology Neurosciences Reports*, 10, 319-326.

Partridge, W.M. (2003) Blood-brain barrier drug targeting: the future of brain drug development. *Molecular Interventions*, 3, 90-105.

Partridge, W.M. (2005) The blood-brain barrier: bottleneck in brain drug development. *NeuroRx*, 2, 3-14.

Perisic-Janjic, N.; Kaliszan, R.; Wiczling, P.; Milosevic, N.; Uscumlic, G.; Banjac, N. (2011) Reversed-phase TLC and HPLC retention data in correlation studies with in silico molecular descriptors and drug likeness properties of newly synthesized anticonvulsant succinimide derivatives. *Molecular Pharmaceutics*, 8:555-563.

Potschka, H. (2012) Role of CNS efflux drug transporters in antiepileptic drug delivery: Overcoming CNS efflux drug transport. *Advanced Drug Delivery Reviews*, 64, 943-952.

Rogawski, M.A. (2006) Diverse mechanisms of antiepileptic drugs in the development pipeline. *Epilepsy Research*, 69, 273-294.

Schmidt, D. (2011a) Efficacy of new antiepileptic drugs. *Epilepsy Currents*, 11, 9-11.

Schmidt, D. (2011b) Antiepileptic drug discovery: does mechanism of action matter? *Epilepsy Behaviour,* 21, 342-343.

Spina, E. (2002) Carbamazepine – chemistry, biotransformation and pharmacokinetics. In: R.H. Levy, R.H Mattson, B.S. Meldrum, E. Perucca (Eds.), *Antiepileptic drugs* (pp. 236-246), Philadelphia: Lippincott Williams & Wilkins.

Yengi, L.G.; Leung, L.; Kao, J. (2007) The evolving role of drug metabolism in drug discovey and development. *Pharmaceutical Research*, 24, 842-858.

Zhao R.; Kalvass J.C.; Pollack, G.M. (2009) Assessment of blood-brain barrier permeability using the in situ mouse brain perfusion technique. *Pharmaceutical Research*, 26, 1657-1664.

Figure captions

Fig. 1 Chemical structures of the dibenz[*b*,*f*]azepine-5-carboxamide derivatives investigated in the present study: CBZ, CBZ-E, OXC, *S*-Lic, *R*- Lic, *trans*-diol, ESL, BIA 2-059, BIA 2-024 and BIA 2-265.

Fig. 2 Plasma concentration-time profiles after the oral administration of a single equimolar dose (1.4 mmol/kg), of CBZ (a), CBZ-E (b), OXC (c), ESL (d), *S*-Lic (e), *R*-Lic (f), *trans*-diol (g), BIA 2-059 (h), BIA 2-024 (i) and BIA 2-265 (j) to mice. Symbols represent the mean values ± standard error of the mean of four determinations per time point ($n = 4$)

Fig. 3 Brain concentration-time profiles after the oral administration of a single equimolar dose (1.4 mmol/kg) of CBZ (a), CBZ-E (b), OXC (c), ESL (d), *S*-Lic (e), *R*-Lic (f), *trans*-diol (g), BIA 2-059 (h), BIA 2-024 (i) and BIA 2-265 (j) to mice. Symbols represent the mean values ± standard error of the mean of four determinations per time point ($n = 4$)

Table 1 – Plasma pharmacokinetic parameters of parent compounds and metabolites obtained in mice after the oral administration of a single equimolar dose (1.4 mmol/kg) of CBZ, CBZ-E, OXC, *S*-Lic, *R*- Lic, *trans*-diol, ESL, BIA 2-059, BIA 2-024 and BIA 2-265.

Parent Compound	Parent & Metabolites	Pharmacokinetic Parameters					
		t_{max} (h)	C_{max} (µg/mL)	$AUC_{0\text{-}12h}$ (µg.h/mL)	$AUC_{0\text{-}\infty}$ (µg.h/mL)	$t_{1/2}$ (h)	MRT (h)
CBZ	CBZ	0.50	37.80	162.63	180.20	3.38	4.85
	CBZ-E	4.00	20.40	178.21	414.82	12.52	19.73
CBZ-E	CBZ-E	0.50	44.10	286.39	360.53	4.89	7.93
OXC	OXC	1.00	30.60	191.49	314.74	8.99	12.77
	S-Lic	2.00	4.79	39.98	59.51	6.78	10.75
S-Lic	*S*-Lic	0.25	50.50	159.59	231.41	7.66	10.22
	R-Lic	NA	NA	NC	NC	NC	NC
	OXC	1.00	5.27	32.89	49.48	7.37	10.89
R-Lic	*R*-Lic	0.25	70.20	206.90	214.25	2.43	3.56
	S-Lic	0.50	1.11	5.23	7.96	5.11	7.42
	OXC	0.50	5.44	22.86	25.06	3.39	4.92
Trans-diol	*Trans*-diol	0.50	57.70	379.14	775.27	13.46	18.43
ESL	ESL	0.50	1.59	0.43	NC	NC	NC
	S-Lic	0.25	59.00	245.71	296.13	5.22	6.54
	R-Lic	0.25	0.47	0.64	1.63	2.41	3.72
	OXC	2.00	8.31	49.70	56.00	3.55	5.70
BIA 2-059	BIA 2-059	NA	NA	NC	NC	NC	NC
	S-Lic	0.25	0.83	3.03	3.26	2.02	3.22
	R-Lic	0.25	83.60	268.96	310.65	3.99	5.65
	OXC	2.00	5.02	30.81	43.04	6.84	9.57
BIA 2-024	BIA 2-024	2.00	58.10	331.29	373.37	3.43	5.28
	S-Lic	0.25	0.25	0.03	NC	NC	NC
	R-Lic	8.00	0.64	4.53	NC	NC	NC
BIA 2-265	BIA 2-265	0.25	28.00	10.39	11.97	1.29	1.51

AUC, area under the plasma drug concentration-time curve; C_{max}, peak concentration; t_{max}, time to reach peak concentration; $t_{1/2}$, apparent terminal elimination half-life; MRT, mean residence time; NA, not available; NC, not calculated

Table 2 – Brain pharmacokinetic parameters of parent compounds and metabolites obtained in mice after the oral administration of a single equimolar dose (1.4 mmol/kg) of CBZ, CBZ-E, OXC, *S*-Lic, *R*- Lic, *trans*-diol, ESL, BIA 2-059, BIA 2-024 and BIA 2-265

Parent Compound	Parent & Metabolites	Pharmacokinetic Parameters					
		t_{max} (h)	C_{max} (µg/g)	AUC_{0-12h} (µg.h/g)	$AUC_{0-\infty}$ (µg.h/g)	$t_{1/2}$ (h)	MRT (h)
CBZ	CBZ	2.00	28.02	141.78	149.07	2.48	3.86
	CBZ-E	4.00	12.24	106.10	173.42	7.78	12.78
CBZ-E	CBZ-E	0.50	30.25	232.63	286.00	4.80	7.62
OXC	OXC	1.00	22.32	158.99	254.55	8.66	12.32
	S-Lic	4.00	2.10	17.46	28.17	7.45	12.24
S-Lic	*S*-Lic	2.00	12.61	87.09	116.43	5.95	8.76
	R-Lic	NA	NA	NC	NC	NC	NC
	OXC	1.00	2.74	27.17	76.79	20.47	28.92
R-Lic	*R*-Lic	2.00	7.44	53.99	59.12	3.08	5.33
	S-Lic	NA	NA	NC	NC	NC	NC
	OXC	2.00	1.81	12.95	16.17	5.20	7.79
Trans-diol	*Trans*-diol	4.00	10.79	102.79	271.62	15.52	23.65
ESL	ESL	0.50	1.34	0.32	NC	NC	NC
	S-Lic	2.00	18.30	99.80	117.61	4.37	6.23
	R-Lic	NA	NA	NC	NC	NC	NC
	OXC	2.00	6.93	41.05	47.01	3.78	5.92
BIA 2-059	BIA 2-059	NA	NA	NC	NC	NC	NC
	S-Lic	0.50	0.28	0.35	0.47	0.88	1.54
	R-Lic	0.50	15.57	58.29	73.70	5.74	7.43
	OXC	1.00	3.03	14.54	22.41	8.79	11.55
BIA 2-024	BIA 2-024	2.00	20.85	116.27	131.40	3.39	5.49
	S-Lic	NA	NA	NC	NC	NC	NC
	R-Lic	8.00	0.64	4.53	NC	NC	NC
BIA 2-265	BIA 2-265	4.00	0.31	0.51	NC	NC	NC

AUC, area under the plasma drug concentration-time curve; C_{max}, peak concentration; t_{max}, time to reach peak concentration; $t_{1/2}$, apparent terminal elimination half-life; MRT, mean residence time; NA, not available; NC, not calculated

Table 3 – Brain/plasma C_{max} and $AUC_{0-\infty}$ of CBZ, CBZ-E, OXC, *S*-Lic, *R*- Lic, *trans*-diol, ESL, BIA 2-059, BIA 2-024 and BIA 2-265 obtained after oral gavage administration of each compound to mice at 1.4 mmol/kg.

Parent Compound	Parent & Metabolites	Brain/Plasma Ratio		
		C_{max}	AUC_{0-12h}	$AUC_{0-\infty}$
CBZ	CBZ	0.74	0.87	0.83
	CBZ-E	0.60	0.59	0.42
CBZ-E	CBZ-E	0.69	0.81	0.79
OXC	OXC	0.73	0.83	0.81
	S-Lic	0.44	0.44	0.47
S-Lic	*S*-Lic	0.25	0.55	0.50
	R-Lic	NA	NC	NC
	OXC	0.52	0.88	1.55
R-Lic	*R*-Lic	0.11	0.26	0.28
	S-Lic	NA	NC	NC
	OXC	0.33	0.57	0.65
Trans-diol	*trans*-diol	0.19	0.27	0.35
ESL	ESL	0.84	0.74	NC
	S-Lic	0.31	0.41	0.40
	R-Lic	NA	NC	NC
	OXC	0.83	0.83	0.84
BIA 2-059	BIA 2-059	NA	NC	NC
	S-Lic	0.34	0.12	0.15
	R-Lic	0.19	0.22	0.24
	OXC	0.60	0.47	0.52
BIA 2-024	BIA 2-024	0.36	0.35	0.35
	S-Lic	NA	NC	NC
	R-Lic	1.0	1.0	NC
BIA 2-265	BIA 2-265	0.01	0.05	NC

AUC, area under the plasma drug concentration-time curve; C_{max}, peak concentration; NA, not available; NC, not calculated

Table 4 – Percentage of binding of CBZ, CBZ-E, OXC, *S*-Lic, *R*- Lic, *trans*-diol, ESL, BIA 2-059, BIA 2-024 and BIA 2-265 to mouse plasma proteins using the ultrafiltration method. Values represent mean ± standard deviation (n = 4)

Compound	Concentration (μM)	Binding (%)
CBZ	40.0	71.61 ± 3.19
CBZ-E	4.0	47.86 ± 3.61
OXC	8.0	76.56 ± 3.24
***S*-Lic**	100.0	28.70 ± 1.10[a]
***R*-Lic**	100.0	31.50 ± 1.60[a]
***Trans*-diol**	15.0	23.02 ± 4.29
ESL	6.0	58.38 ± 2.62
BIA 2-059	6.0	64.42 ± 5.28
BIA 2-024	100.0	32.27 ± 9.32
BIA 2-265	100.0	89.39 ± 4.87

[a] Obtained from Fortuna et al (2010).

Table 5 Values of MM, pKa, logP and PSA for CBZ, CBZ-E, OXC, ESL, *S*-Lic, *R*-Lic, *trans*-diol, BIA 2-059, BIA 2-024 and BIA 2-265

Compound	**MM** (g/mol)	**pKa**	**LogP**	**PSA** ($Å^2$)
CBZ	236.3	13.9	2.67	46.3
CBZ-E	252.3	NF	1.26	36.1
OXC	252.3	13.7; 10.0	1.54	63.4
***S*-Lic**	254.3	14.1; 13.8	0.98	66.6
***R*-Lic**	254.3	14.1; 13.8	0.98	66.6
***Trans*-diol**	270.3	14.4; 12.9	0.13	86.8
ESL	296.3	14.0	1.70	72.6
BIA 2-059	296.3	14.0	1.70	72.6
BIA 2-024	267.3	13.9; 11.2	0.91	78.9
BIA 2-265	313.3	14.6; 13.7	1.51	112.4

NF, not found

Highlights

First *in vivo* evaluation of systemic and brain pharmacokinetics of ten CBZ analogs;

CBZ, CBZ-E and OXC presented the highest values of brain/plasma ratios;

Plasma protein binding seems to compromise the brain penetration if higher than 90%;

New ADME data of CBZ analogues to support the development of *in silico* models.

Figure(s)

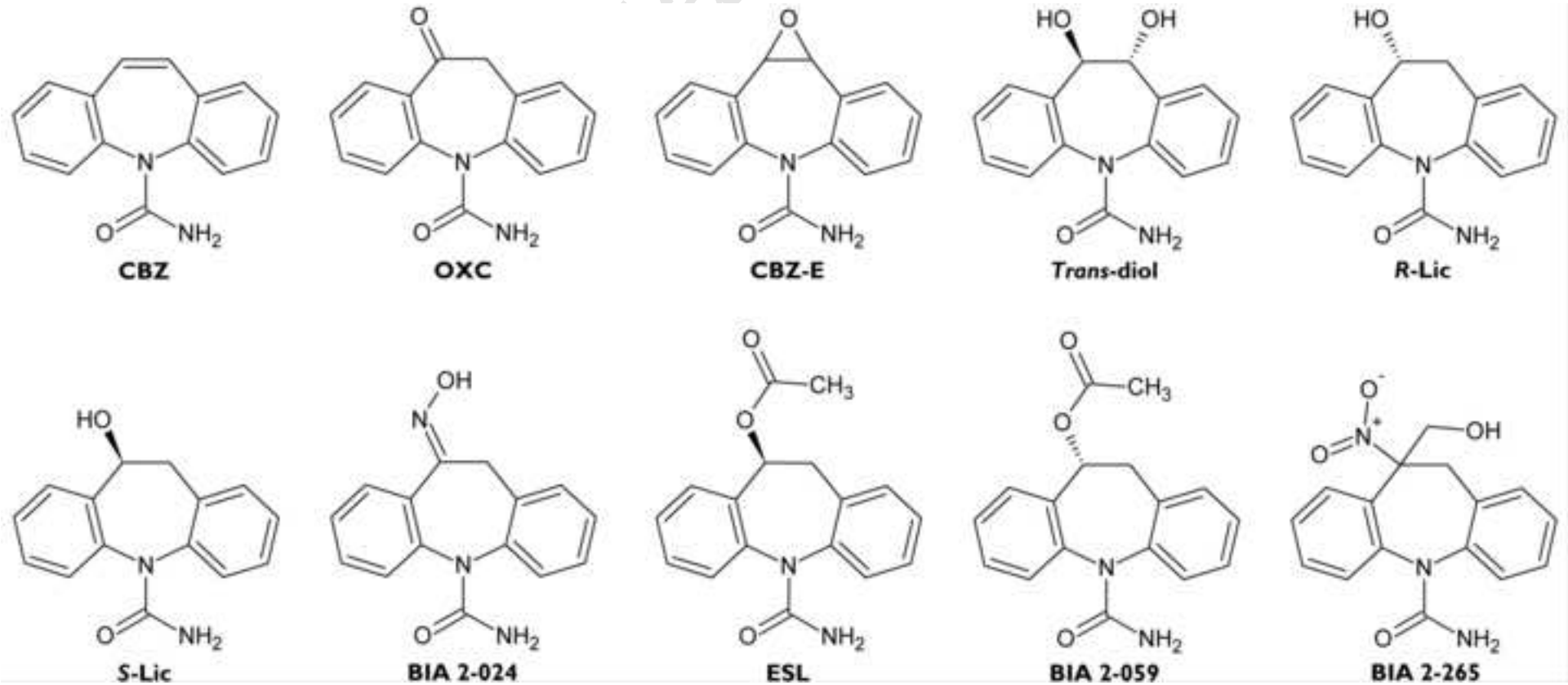
CBZ
OXC
CBZ-E
Trans-diol
R-Lic
S-Lic
BIA 2-024
ESL
BIA 2-059
BIA 2-265